COMPUTER-AIDED DESIGN & APPLICATIONS, 2018
VOL. 15, NO. 5, 677–683
https://doi.org/10.1080/16864360.2018.1441235

Mesh segmentation via geodesic curvature flow

Zhiyu Sun [a], Ramy Harik [b] and Stephen Baek [a]

[a]The University of Iowa, USA; [b]University of South Carolina, USA

ABSTRACT

Perceptually meaningful segmentation of a mesh is one of the fundamental, yet unconquered problems in computer-aided design and geometry modeling. A critical component that affects the result of segmentation is a similarity metric, which quantifies how likely two distinct points belong to the same segment. Traditionally, similarity metrics were defined based on analytic properties of a surface geometry such as the curvature. Although these metrics work well in dividing segments based on creases and ridges, they provide unsatisfactory results in volumetric intersections between two large chunks. To this end, in this paper, we present a novel method for improving any given similarity metric in a way that is more suitable for segmentation tasks. We introduce the geodesic curvature flow, which is a geometric flow that minimizes the arc length of level set contours, to evolve the original similarity metric into a new metric. In our study, the new metric was discovered to be more suitable for the segmentation tasks than the original metric in a sense that it compensates the aforementioned limitations.

KEYWORDS

Geodesic curvature flow; geometric flow; surface metric; mesh segmentation

1. Introduction

Triangular mesh segmentation [16] is one of the fundamental problems in computer-aided design and geometry modeling. The problem can be briefly stated as a task of finding a partition S of a triangular mesh X. Mathematically, a partition S of a set X is a disjoint collection of nonempty and distinct subsets of X such that each element of X is an element of some, and hence, exactly one element of S [18]. Intuitively, there can be more than one such a collection for a given X, and the problem of mesh segmentation is, hence, to find the most *perceptually sound* partition of a given mesh X. Albeit ambiguous, the "perceptually sound" segmentation is determined, most of the time, through a visual comparison to find the most natural segmentation to our common intuition.

A critical component for distilling the perceptual soundness of a segmentation into a numerical algorithm is the similarity metric. The similarity metric is a measure of how visually similar and contiguous the elements are, and thus, how likely they belong to the same segment. It provides a numerical tool for comparing the elements of a geometry. Many of the segmentation methods (see Sec. 2) utilize some inherent measures that can be computed directly from the mesh, for example, dihedral angles between the faces, curvatures, and such. These measures often provide a reasonable fidelity of segmentation since the human visual perception relies largely on surface curvatures [4][11]. However, at the same time, these are not capable of embracing geometric characteristics in a global, volumetric scope, such as narrow necks (i.e., regions where cross-sectional area reduces rapidly) or intersections between large chunks of geometries, when there is no prominent marks of creases and ridges on the surface.

In our recent study, we discovered that, given a similarity metric of any kind, the geodesic curvature flow (GCF) significantly improves the metric in a way that better conforms to the rules and the intuitions of visual segmentation (see Fig. 1). In fact, the GCF, which is essentially a geometric flow of a scalar function on a manifold, showed in our experiment a strong tendency of improving a given similarity metric in a form of the distance function that satisfies important rules and principles of human visual cognition, such as minima rule [11]. Therefore, in this paper, we propose a novel framework of utilizing the GCF for more perceptually sound segmentation of 3D mesh. We review some of the previous approaches in mesh segmentation (Sec. 2), present mathematical backgrounds of the GCF (Sec. 3), and discuss the result of segmentation improved by the GCF (Sec. 4).

CONTACT Zhiyu Sun zhiyu-sun@uiowa.edu; Ramy Harik harik@cec.sc.edu; Stephen Baek stephen-baek@uiowa.edu

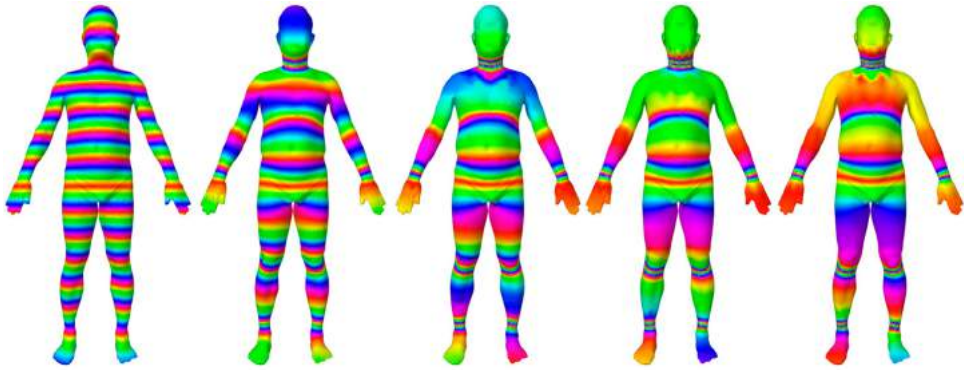

Figure 1. Evolution of a level set function under the geodesic curvature flow (from left to right). Each of the figures corresponds to the result after 0, 5, 20, 100, and 500 iterations respectively. The time step is set to h = 10. For the details on the parameters, see Sec. 3.3.

2. Related works

Mesh segmentation aims to decompose a surface mesh into perceptually meaningful partitions. In order to achieve such task, a large variety of computational methods has been proposed so far. Among those different approaches, one of the key challenges they share in common is to define a metric quantifying the dissimilarity between points on the surface.

Katz *et al.* [10] proposed an algorithm to compute a hierarchical decomposition of a given mesh. In their approach, the probability of a face belongs to a certain segment depends on its distance from other faces in this segment. They also used the dihedral angle between two adjacent facets in addition to the geodesic distance to help define the likeliness of the two facets belonging to the same segment. Page *et al.* [14] developed a hill climbing watershed algorithm for segmenting a triangular mesh into visual parts. In their implementation, they precomputed the principal curvatures and their principal directions at each vertex of a mesh. The principal curvature values was used as a metric to set the threshold for the watershed clustering in the algorithm.

More recently, a group of shape descriptors developed based on the spectrum of the Laplace-Beltrami operator [15],[19],[1] has gained a significant spotlight in the research of mesh segmentation. Rustamov [15] introduced the global point signature (GPS) which encodes the geometry information about a point on the surface. The GPS at each point on the surface was defined as a vector containing the Laplace eigenfunctions of different modes scaled by the corresponding eigenvalues. The Euclidean distance between such vectors was defined as the similarity metric between two points on the surface. In [15], it was shown that the GPS distance can serve as a good similarity metric for the segmentation tasks. The heat kernel signature (HKS), another spectral shape descriptor based on the different heat diffusion characteristics according to the shape of a surface, was proposed by Sun *et al.* [19]. Skraba *at al.* [17] presented a persistence-based segmentation technique using the HKS. In their algorithm, the HKS function at each point on the mesh for a user-defined time value t was used to guide the persistence-based clustering, which results in an isometry-invariant multi-scale segmentation. In [7] and [22], HKS was also further developed or modified to tailor the clustering task depending on specific applications. In a similar spirit with HKS, Aubry *et al.* [1] proposed the wave kernel signature (WKS) based on a characterization of the wave propagation on manifolds. Physically, the WKS represents the average probability of measuring a quantum mechanical particle at a surface point. Mathematically, the WKS is another expression in the eigenfunctions of the Laplace-Beltrami operator, and essentially similar to the GPS and HKS. In [1], the WKS value at each point on the mesh was used as the guidance to group those points. For pose-consistent 3D shape segmentation tasks, the WKS metric-based method was reported to be more robust to data perturbed by various kinds of noise.

A commonly shared problem of the existing methods is that they tend to ignore geometric characteristics in a global, volumetric scope. In turn, narrow necks or intersections between large chunks of volumes are often ignored unless there is a prominent mark of creases and ridges on the surface. This is critical for the intuitive segmentation of a shape, because, for the segmentation and abstraction of shapes, human cognition depends largely on a volumetric composition of shapes in a global scope.

Motivated from this, we propose in this paper a novel method for deriving a shape-aware surface metric using the GCF. We have found from experiments that the GCF has a strong tendency of improving a given similarity metric in such a way that reflects the global, volumetric composition of shapes more intuitively. For a given

similarity metric of any kind, whether it be the geodesic distance, GPS, HKS, WKS, or any other, the GCF can significantly improve the initial metric in a way that better conform to the rules and the intuitions of visual cognition.

3. The method

A brief overview of the method is as follows. First, the geodesic distance between every pair of vertices on an input mesh X is computed as our initial surface metric. We then evolve the surface metric via the GCF in order to achieve better measurement for the clustering task. Using the eigenfunctions of the new metric, we find the spectral embedding of X. Finally, we cluster the vertices on the spectral configuration, which gives a visually intuitive segmentation of X. The new metric essentially is an indicator of how likely two distinct points are in the same segment. Hence, the spectral embedding will lead to a projection of X onto a higher dimensional space such that the distances between the points are reconfigured according to their likeliness of belonging to the same segment. Relevant literatures report that well-known metrics (e.g., Euclidean distance, geodesic distance) perform well for such a segmentation method based on a spectral embedding [12][13], but we found that a new metric achieved by evolving the geodesic distance via the geodesic curvature flow performs much better than the conventional metrics. In this section, we introduce and define the GCF (Sec. 3.1), discuss how the GCF can be utilized for evolving the similarity metric for the clustering (Sec. 3.2), and discretize the GCF on a triangular mesh domain without loss of generality (Sec. 3.3).

3.1. Geodesic curvature flow

The geodesic curvature flow (GCF) is a geometric flow, or informally, a continuous evolution of a curve that minimizes the arc length of a curve. Given a closed self-avoiding rectifiable curve γ lying on a differential d-manifold $\mathfrak{M}$ embedded in $\mathbb{R}^n (d \leq n)$, the energy functional of the GCF is defined as follows:

$$E(\gamma) = \int_{\gamma} dl \tag{3.1}$$

where dl is an infinitesimal segment defined on the curve γ for the integration. Here, we restrict our curve to be rectifiable in order to make sure that it is integrable. A curve γ on a manifold $\mathfrak{M}$ is said to be *rectifiable* if and only if the length of every geodesic polygon formed by vertices $\gamma(t_1), \ldots, \gamma(t_n)$, $0 \leq t_1 < \cdots < t_n \leq 1$ can be bounded from above by the length of the curve for some parameterization $\gamma(t)$, $t \in [0, 1]$ and under the induced metric of $\mathfrak{M}$. This consequently means that the curve γ is a function with bounded variations, and thus integrable.

In a level set formulation, the energy functional in Eqn. (3.1) is converted from a line integral to a surface integral on a manifold by the coarea formula [6]:

$$E(\gamma) = \int_{\mathfrak{M}} \delta(\phi) |\nabla \phi| dA \tag{3.2}$$

where ϕ is a level set formulation of the curve γ such that the contour of $\phi = 0$ is equal to γ and dA being an infinitesimal area defined on the manifold $\mathfrak{M}$. δ is the Dirac's delta function. Consequently, the energy functional in Eqn. (3.2) can further be reduced to the Euler-Lagrange partial differential equation:

$$-\nabla \cdot \frac{\nabla \phi}{|\nabla \phi|} \delta(\phi) = 0 \tag{3.3}$$

$$\left. \frac{\partial \phi}{\partial n} \right|_{\partial \mathfrak{M}} = 0 \tag{3.4}$$

where $\partial \mathfrak{M}$ is the boundary of $\mathfrak{M}$ and n is the outward normal at the boundary. For closed $\mathfrak{M}$, the boundary condition is ignored automatically.

Further, for the discretization, we introduce a so-called "smoothed out" delta function, $\delta(\phi) = |\nabla \phi|$ as like in the standard level set methods to obtain the following gradient descent flow:

$$\frac{\partial \phi}{\partial t} = \nabla \cdot \frac{\nabla \phi}{|\nabla \phi|} |\nabla \phi| \tag{3.5}$$

Time integration of Eqn. (3.5) provides us the "evoloved" level set function $\phi(t)$ of the original function ϕ_0. Fig. 1 shows such an evolution of a level set function defined on a human model. An interesting behavior of the GCF is that it "diffuses" and smooths out the level set function except for the narrow necks of the manifold. This property can also be observed from Fig. 1, in which the level set function is smoothed out, and hence, the function value does not change much over the large, continuous areas; whereas the level set contours are converged around relatively narrow parts such as neck, wrists, knees, ankles, waist, and so on, and hence, the function value changes relatively faster. Therefore, if the level set function was a surface distance from a certain point p (the top of the head in Fig. 1), then the evolved function under the GCF would be a better metric for the segmentation tasks, which is our insight for the proposed method in this paper.

3.2. Geometry-aware metric via geodesic curvature flow

As aforementioned, one of the characteristics of the GCF is that it tends to evolve faster on large, continuous areas

and significantly slower on narrow areas. Especially, level set curves under the GCF tend to converge near the shortest homotopic cycles. Our key insight here is to exploit such a characteristic of the GCF to evolve the distance metric on the surface in aware of the geometric contiguity.

To achieve so, we first start with the geodesic distance $d(p,x)$ from a given point p on the manifold surface $\mathfrak{M}$. We then substitute $\phi(x) = d(p,x)$ in Eqn. (3.5) and integrate along certain time t to obtain a new distance function r:

$$r(p,x) := \phi_t(x) = \int_0^t \nabla \cdot \frac{\nabla\phi}{|\nabla\phi|}|\nabla\phi|dt \tag{3.6}$$

Note here that the initial computation of the geodesic distance function d does not have to be the exact geodesics, since d converges to r under the GCF in a fairly robust manner despite of small minor variations of the function values. This allows the use of fast approximate methods for the computation of the geodesic distance, such as [5], or even, the simple Euclidean distance.

For the spatial discretization, we simply assumed that the function value changes linearly on each of the triangular facets in the mesh. Based on this, gradient and divergence operators are defined as finite difference operators similar to the ones used in [5]. For the time discretization, we used the implicit Euler method.

We repeat this process for every vertex v_i in the mesh to obtain a distance matrix R whose elements are $R(i,j) = r(v_i, v_j)$. The distance matrix R is initially not symmetric, since there is no mechanism of restricting the GCF to retain the symmetry $r(x,y) = r(y,x)$. Hence, we make R symmetric simply by updating it to $R \leftarrow \frac{1}{2}(R + R^T)$ in a favor of computational simplicity, where R^T is the matrix transpose of R. Note that more rigorous symmetrization techniques such as [8] could also be utilized, but there we found there was not much difference in the final segmentation result.

3.3. Implementation

3.3.1. Temporal discretization of GCF

Let us write G and D to denote, without specification at the moment, the discrete gradient and divergence operators respectively. Based on this notation, Eqn. (3.5) is expressed in a matrix form as follows w.l.o.g.:

$$\frac{\partial\Phi}{\partial t} = SDMG\Phi \tag{3.7}$$

where Φ is a vector containing function values of ϕ, and S and M are diagonal matrices whose elements are $|\nabla\phi|$ and $\frac{1}{|\nabla\phi|}$ respectively.

In this setup, we apply the backward Euler method for the temporal discretization of Eqn. (3.5) as follows:

$$\left.\frac{\partial\Phi}{\partial t}\right|_t \approx \frac{\Phi_{t+h} - \Phi_t}{h} = SDMG\Phi_{t+h} \tag{3.8}$$

Note that the use of the backward Euler is for the sake of simplicity, and hence, that the other discretization methods such as Runge-Kutta method can also be used in solving the problem.

Consequently, from Eqn. (3.8), we arrive to the following linear system for updating the function ϕ at time a given time t by the time step h:

$$\Phi_{t+h} = (I - hSDMG)^{-1}\Phi_t \tag{3.9}$$

3.3.2. Discretization of differential operators

From among the several possible discretization strategies of the differential operators, we employ the results derived from the discrete exterior calculus [9], which provides a rigorous mathematical discretization of the differential operators on a triangular mesh. This is the most common choice in the field of computational geometry because of its simplicity and relatively reliable performance. However, the other discretization methods (e.g., [21]) could also be utilized. Note that our method is not dependent upon the choice of the discretization of the differential operators.

The Discrete gradient operator associated with each triangle, acting on scalar valued functions defined at each vertex is defined as follows:

$$\nabla\phi = \frac{1}{2A_f}\sum_i \phi_i(N \times e_i) \tag{3.10}$$

where e_i is the edge vector opposing the vertex i, N is the unit normal to the face, and A_f is the area of the face. The sum is taken over the vertices in the given face.

In addition, the discrete divergence operator associated with a given vertex acting on vector fields defined at each triangle is defined as follows:

$$\nabla \cdot X = \frac{1}{2}\sum_j \cot\theta_1(e_1 \cdot X_j) + \cot\theta_2(e_2 \cdot X_j) \tag{3.11}$$

where e_1, e_2 are the edge vectors emanating from the vertex i, and θ_1, θ_2 are the interior angles opposing the edge vectors accordingly. The sum is taken over the incident faces to the vertex i.

The above definitions of the discrete gradient and divergence operators on a triangular mesh allows expressions using matrices $G \in \mathbb{R}^{3|F|\times|V|}$ and $D \in \mathbb{R}^{|V|\times 3|F|}$ respectively. These notations are consistent with what have been used in Section 3.3.1.

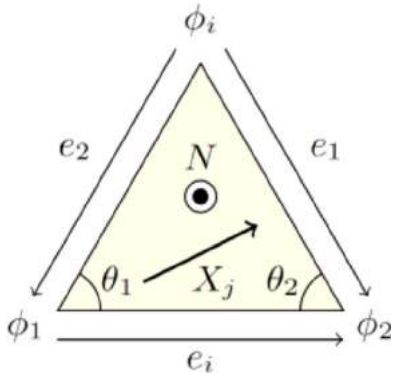

Figure 2. Notations used to define the differential operators on triangular meshes.

3.3.3. Spectral embedding and clustering

Spectral embedding is a commonly used technique for projecting a manifold embedded in $\mathbb{R}^n$ to a different mathematical space S, with applications such as nonlinear dimensionality reduction [20], surface parameterization [23], and so on. Similarly to [13], we utilize spectral embedding to facilitate the clustering task. To do so, we first compute the affinity matrix W using the Gaussian kernel:

$$W(i,j) = e^{-R^2(i,j)/2\sigma^2} \tag{3.12}$$

Note here that $W(i,j)$ varies, by definition, in the range $(0,1]$ depending on the likeliness between two vertices v_i and v_j. In addition, from the inherent nature of the Gaussian kernel, $W(i,j)$ drops significantly towards zero when $R(i,j) > 2\sigma$. Therefore, we simply cutoff values outside 2σ to zero to achieve a highly sparse affinity matrix $W(i,j)$, which has a significant numerical advantage for the computation over the original dense matrix.

The affinity matrix is then normalized to $N = \Sigma^{-1/2} W \Sigma^{-1/2}$ in order to eliminate the effect of different vertex densities, where Σ is a diagonal matrix each of whose elements is the sum of the corresponding row of W, i.e., $\Sigma(i,i) = \sum_j W(i,j)$.

Finally, we compute the spectral embedding of the mesh by performing the eigendecomposition of the normalized affinity matrix N. That is, when we write $\lambda_1, \lambda_2, \ldots, \lambda_K$ as the K-largest eigenvalues eigenvalues of N and $e_1, e_2, \ldots, e_K$ as their associated eigenvectors, the spectral embedding of the mesh is then represented as $Y = \Lambda^{1/2} E$, where Λ is a K-by-K diagonal matrix whose elements are $\lambda_1, \lambda_2, \ldots, \lambda_K$ and $E = \begin{bmatrix} e_1 & e_2 & \cdots & e_K \end{bmatrix}$. Here, Ycan be thought of as a new coordinate matrix in K-dimensional space for the vertices of the mesh. The new embedding, Y brings the similar points closer while it pulls the dissimilar points further apart [3]. Therefore, the clustering task in the spectral embedding is easier and more robust than that in the original embedding.

4. Result

Using the proposed method, we computed segmentation for a number of benchmark models. Fig. 3 shows the result of segmentation performed on the benchmark models using the evolved metrics via GCF, in comparison with the original distance metrics. All of the results were generated using a time step $h = 100$ and the total of 100 iterations.

Segmentation results were significantly improved when the proposed GCF metrics are used compared to the original distance metrics. From Fig. 3, it is clear that the objects are segmented in a more intuitive way via the utilizing of the GCF metric. For example, segmentation of the ears of the Stanford bunny was more intuitive and perceptually reasonable when the GCF metric was used compared to the original cases. Such an improvement could also be observed from the other models. For instance, the segmentation results of the human model have been improved by the GCF in both the geodesic distance and the GPS distance cases. It could be observed that the segments around the torso were significantly improved in such a way that makes more sense with respect to anthropometrical intuition.

In fact, the level set contours of a function under the GCF tend to shrink down in terms of the arc length. Therefore, the level set contours, i.e., the equidistance levels, tend to converge to the locally shortest homotopic cycle on a surface under the GCF. Hence, in turn, a similarity metric under the GCF tends to develop more equidistance levels near the "neck" areas or the regions with the locally minimum cross section. This, in other words, means that the distance from a point gets rapidly further around the neck areas and therefore, the clustering algorithm can better discriminate visually different chunks of volumes around such areas. Therefore, for a given similarity metric of any kind, the GCF is able to improve the metric in a way that better conforms to the rules and the intuitions of visual segmentation. The result presented in Fig 3 shows the significant improvements of the segmentation by evolving any given metric (Geodesic Distance & GPS Distance) via GCF.

Lastly, in terms of computational speed, the GCF showed a reasonable performance. For all of the experiments presented in the paper, we used an Intel® Core™ i7-4770 CPU 3.40 GHz personal computer with 16.0 GB RAM. The code was implemented and tested in MATLAB R2016b. The computational time varied depending on the number of vertices in the input mesh. The average computational time at one vertex per iteration is from

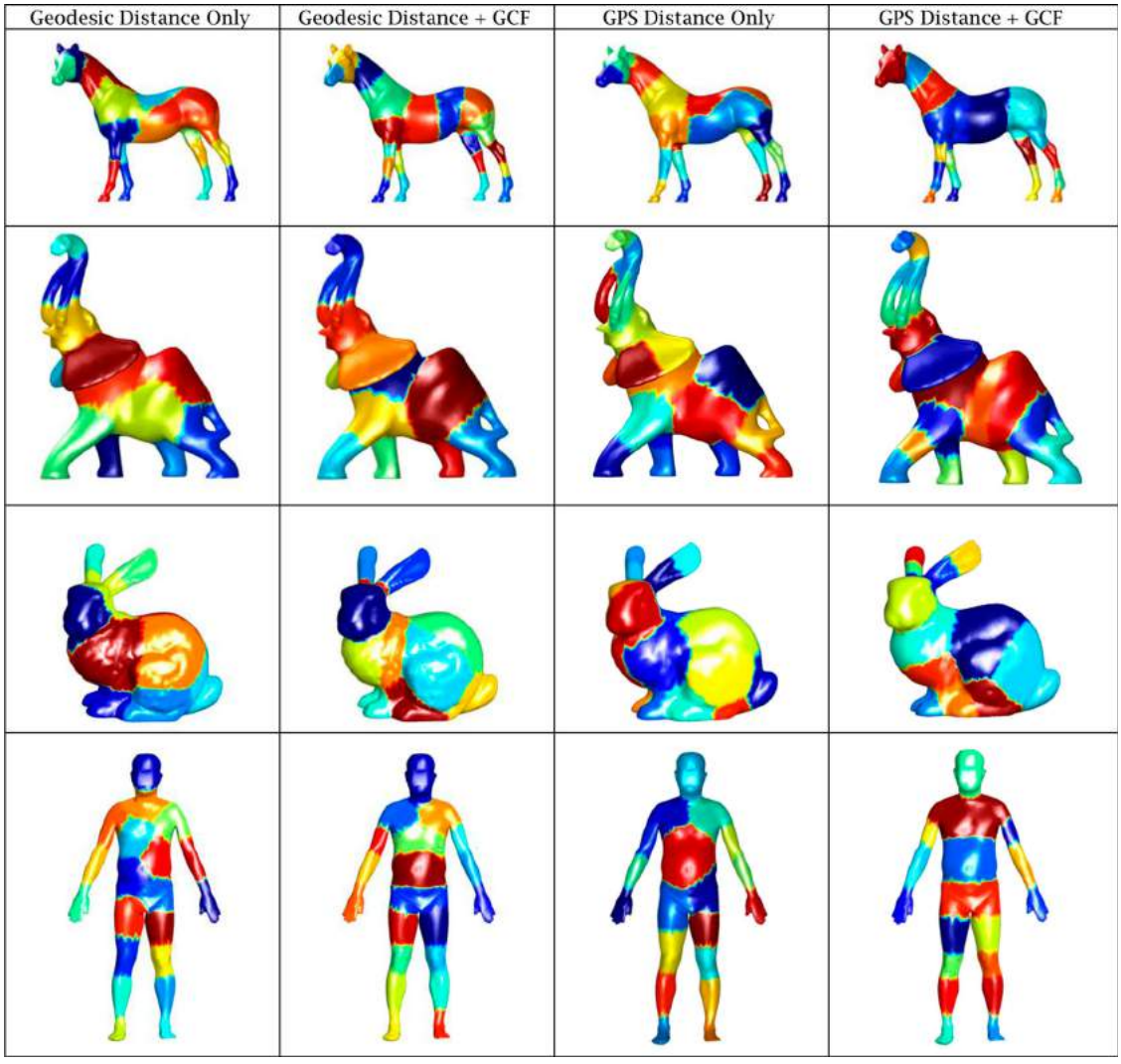

Figure 3. Comparison of the spectral segmentation method with the given similarity metrics (first and third columns) and the improved metric via the GCF (second and fourth columns).

Table 1. Average computational time at one vertex per iteration of models with different mesh sizes

Horse_2500 vertices	Elephant_5000 vertices	Bunny_10000 vertices	Human_5000 veritices
3.123 ms	12.35 ms	27.52 ms	10.67 ms

3.123 to 27.52 millisecond as the number of vertices of different models increasing from 2,500 to 10,000. This result is summarized in the Tab. 1.

5. Conclusion

In this paper, we presented a novel method for the segmentation of a 3D mesh that utilizes the GCF. The GCF-induced metric was preferable for the segmentation tasks in a sense that it provides a better *shape-awareness* for the dissimilarity measure. In addition, even though we demonstrated the results only on the triangular meshes, the method can be generalized to any 3D geometry domain, since our formulation does not assume any particular domain. Instead, as long as there is a well-defined differential operators (i.e., gradient and divergence), our method can be seamlessly scaled to different domains including the parametric surfaces, point clouds, and polygonal meshes (see e.g., [5]).

Despite of the satisfactory performance of our method, it could struggle for the tasks that requires the surface segmentation with respect to small ridges and valleys, as the GCF tends to ignore such features. In this regard, a mathematical insight to improve our method is to introduce an additional weight function $\beta$to the GCF energy $E(\gamma)$. For the GCFs, the weight function acts as a "stopping function" that makes the flow relatively slower than the other areas. Therefore, by introducing β composed of the terms related to the principal curvature

values, we could improve the distance metric even further, which will be our future work. In addition, since the new metric possesses a good shape-awareness, a shape descriptor that encodes the geometric characteristics into a set of numerical values could be developed in the similar spirit of e.g., [15].

ORCID

Zhiyu Sun http://orcid.org/0000-0002-9280-9258
Ramy Harik http://orcid.org/0000-0003-1452-9653
Stephen Baek http://orcid.org/0000-0002-4758-4539

References

[1] Aubry, M.; Schlickewei, U.; Cremers, D.: The wave kernel signature: a quantum mechanical approach to shape analysis, In Proceedings of 2011 IEEE International Conference on Computer Vision Workshops (ICCV Workshops), 2011.
[2] Aubry, M.; Schlickewei, U.; Cremers, D.: Pose-consistent 3D shape segmentation based on a quantum mechanical feature descriptor, In Proceedings of Joint Pattern Recognition Symposium, 2011, 122-131.
[3] Brand, M.; Huang, K.: A unifying theorem for spectral embedding and clustering, TR2002-42, Mitsubishi Electric Research Laboratories, Cambridge, MA, 2002, http://www.merl.com/publications/docs/TR2002-42.pdf.
[4] Cohen, E. H.; Singh, M.: Geometric determinants of shape segmentation: tests using segment identification, *Vision Research*, 47, 2007, 2825-2840. https://doi.org/10.1016/j.visres.2007.06.021
[5] Crane, K.; Weischedel, C.; Wardetzky, M.: Geodesics in heat: a new approach to computing distance based on heat flow, *ACM Transactions on Graphics*, 32(5), 2013, Article No. 152. https://doi.org/10.1145/2516971.2516977
[6] Federer, H.: Geometric Measure Theory, Classics in Mathematics, Springer-Verlag Berlin Heidelberg, 1996.
[7] Harik, R.; Shi, Y.; Baek, S.: Shape Terra: mechanical feature recognition based on a persistent heat signature, *Computer-Aided Design & Applications*, 14(2), 2017, 206-218. https://doi.org/10.1080/16864360.2016.1223433
[8] Higham, N. J.: Computing a nearest symmetric positive semidefinite matrix. *Linear Algebra and Its Applications*, 103, 103-118. https://doi.org/10.1016/0024-3795(88)90223-6
[9] Hirani, A. N.: Discrete Exterior Calculus, Ph.D. Thesis, California Institute of Technology, CA, United States, 2003.
[10] Katz, S.; Tal, A.: Hierarchical mesh decomposition using fuzzy clustering and cuts, *ACM Transactions on Graphics*, 22(3), 2003, 954-961. https://doi.org/10.1145/882262.882369
[11] Lim, I. S.; Leek, E. C.: Curvature and the visual perception of shape: theory on information along object boundaries and the minima rule revisited, *Psychology Review*, 119(3), 2012, 668-677. https://doi.org/10.1037/a0025962
[12] Liu, R.: Spectral Mesh Segmentation, Ph.D. Thesis, Simon Fraser University, Burnaby, BC, Canada, 2009.
[13] Liu, R.; Zhang, H.: Segmentation of 3D meshes through spectral clustering, In Proceedings of the 12th Pacific Conference on the Computer Graphics and Applications (PG'04), 2004, 298-305. https://doi.org/10.1109/PCCGA.2004.1348360
[14] Page, D.L.; Koschan, A.F.; Abidi, M.A.: Perception-based 3D triangle mesh segmentation using fast marching watersheds, Proceedings of IEEE Computer Society Conference on Computer Vision and Pattern Recognition (CVPR), 2003. https://doi.org/10.1109/CVPR.2003.1211448
[15] Rustamov, R.: Laplace-Beltrami eigenfuctions for deformation invariant shape representation, In Proceedings of the 5th Eurographics Symposium on Geometry Processing (SGP'07), 2007, 225-233. https://doi.org/10.2312/SGP/SGP07/225-233
[16] Shamir, A.: A survey on mesh segmentation techniques. In *Computer graphics forum*, 27(6), 2008, 1539-1556. https://doi.org/10.1111/j.1467-8659.2007.01103.x
[17] Skraba, P.; Ovsjanikov, M.; Chazal, F.; Guibas, L: Persistence-based segmentation of deformable shapes, In Proceedings of IEEE Conference on Computer vision and Pattern Recognition Workshops (CVPRW), 2010, 45-52. https://doi.org/10.1109/CVPRW.2010.5543285
[18] Stoll, R.R.: *Set Theory and Logic*, Dover Publications, Inc., New York, NY, 1979.
[19] Sun, J.; Ovsjanikov, M.; Guibas, L.: A concise and provably informative multi-scale signature based on heat diffusion, Proceedings of the Symposium on Geometry Processing (SGP'09), 2009, 1383-1392.
[20] Tenenbaum, J.B.; De Silva, V.; Langford, J.C.: A global geometric framework for nonlinear dimensionality reduction, *Science*, 290(5500), 2000, 2319-2323. https://doi.org/10.1126/science.290.5500.2319
[21] Xu, G.: Convergent discrete Laplace-Beltrami operators over triangular surfaces. In Proceedings of IEEE Geometric Modeling and Processing, 2004, 195-204. https://doi.org/10.1109/GMAP.2004.1290041
[22] Yi, F.; Sun, M.; Kim, M.; Ramani, K.: Heat-mapping: a robust approach toward perceptually consistent mesh segmentation. In Proceedings of IEEE Conference on Computer Vision and Pattern Recognition (CVPR), 2011, 2145-2152.
[23] Zhou, K.; Snyder, J.; Guo, B.; Shum, H.-Y.: Iso-charts: stretch-driven mesh parameterization using spectral analysis, In Proceedings of the 2004 Eurographics/ACM SIGGRAPH Symposium on Geometry Processing (SGP'04), 2004, 45-54. https://doi.org/10.1145/1057432.1057439